# Dependence of electronic properties of epitaxial few-layer graphene on the number of layers investigated by photoelectron emission microscopy

H. Hibino,[1] H. Kageshima,[1] M. Kotsugi,[2] F. Maeda,[1] F.-Z. Guo,[2] and Y. Watanabe[2]
[1]*NTT Basic Research Laboratories, NTT Corporation, Atsugi, Kanagawa 243-0198, Japan*
[2]*Japan Synchrotron Radiation Research Institute (JASRI), Sayo, Hyogo 679-5198, Japan*
(Received 7 July 2008; revised manuscript received 5 February 2009; published 30 March 2009)

We used spectroscopic photoemission and low-energy electron microscopy to investigate the electronic properties of epitaxial few-layer graphene grown on 6H-SiC(0001). Photoelectron emission microscopy (PEEM) images using secondary electrons (SEs) and C 1*s* photoelectrons can discriminate areas with different numbers of graphene layers. The SE emission spectra indicate that the work function increases with the number of graphene layers and that unoccupied states in the few-layer graphene promote SE emission. The C 1*s* PEEM images indicate that the C 1*s* core level shifts to lower binding energies as the number of graphene layers increases, which is consistent with the reported thickness dependence of the Dirac point energy.

DOI: 10.1103/PhysRevB.79.125437 PACS number(s): 68.37.Xy, 79.60.−i, 68.37.Nq, 65.40.gh

## I. INTRODUCTION

Recently, few-layer graphene (FLG) has attracted much attention as a material for future electronics.[1] So far, electronic device properties have been investigated for FLG produced in two ways: graphene flakes exfoliated from bulk graphite[1] and epitaxial FLG grown on SiC.[2,3] Epitaxial FLG has the potential to grow on a wafer scale, if the film morphology is better controlled, and is promising for device integration. To make epitaxial FLG applicable, however, we need to establish a reproducible way of forming wide, uniform graphene layers. For this purpose, we have already demonstrated that the number of layers in epitaxial FLG can be determined by low-energy electron microscopy (LEEM) by using quantized oscillations of electron reflectivity.[4,5] *In situ* microscopic determination of the number of graphene layers using LEEM enabled us to investigate the initial stages of graphene growth.[4,6]

Another important aspect to clarify before device applications of epitaxial FLG is to determine how the SiC substrate influences the electronic properties of FLG. The electronic band structures of epitaxial FLG have been investigated in detail using angle-resolved photoelectron spectroscopy (ARPES).[7–13] The Dirac point at the $K$ point falls below the Fermi level,[7–11] and the shift from the Fermi level decreases with the number of graphene layers.[9–11] Electrons are transferred from the SiC substrate to the FLG. The C 1*s* photoelectron spectroscopy (PES) spectra indicated that the C 1*s* core level also shifts to lower binding energies as the number of graphene layers increases.[13] This means that the electronic structure of epitaxial FLG rigidly shifts due to the electron doping. Moreover, it has been reported that the interaction between epitaxial FLG and SiC substrate opens the band gap at the Dirac point,[8,10] but there is still some controversy about the gap opening.[12]

Previous PES studies have clarified various influences of the SiC substrate on the electronic properties of epitaxial FLG. However, because it is still difficult to grow uniform epitaxial FLG with an intended thickness, the spatially averaged PES technique inevitably provides us information weighted by the distribution of the number of graphene layers. It is desirable to investigate the electronic properties using techniques that can resolve the number of layers microscopically. In this work, therefore, we used spectroscopic photoemission and low-energy electron microscopy (SPELEEM). From photoelectron emission microscopy (PEEM) images made of secondary electrons (SEs) and C 1*s* photoelectrons, we can discriminate areas with different numbers of graphene layers. The SE emission spectra indicate that the threshold energy of the SE emission shifts to higher energies with increasing the number of graphene layers and that the spectrum shape depends on the number of graphene layers. The C 1*s* PEEM images confirm the reported result that the C 1*s* core level shifts to lower binding energies as epitaxial FLG thickens.[13]

## II. EXPERIMENT

We measured PEEM images of epitaxial FLG grown on 6H-SiC(0001) using a commercial SPELEEM instrument (Elmitec LEEM III with an energy analyzer) at BL17SU of SPring-8.[14] SPELEEM can be operated in image, diffraction, or dispersion modes by changing the lens parameters. Under the photon irradiation, we obtained PEEM images and emission patterns of photoelectrons in the image and diffraction modes, respectively.[15] The dispersion mode enabled us to directly image the dispersion plane of the energy analyzer on the screen. The photoelectron intensity on the dispersion plane was directly converted to the PES spectra. Using the selected-area apertures, emission patterns and PES spectra from the area down to ~1 μm in diameter could be obtained. The PES spectra were also obtained microscopically from the sequential PEEM images at different energies.

In the SPELEEM instrument, the electron gun was biased at the acceleration voltage $-V$ of about −20 kV and the sample was biased at $-V+V_{\mathrm{ST}}$, where $V_{\mathrm{ST}}$ is the start voltage. The electron-beam energy $E^{\mathrm{beam}}$ from the ground level is close to $eV+W_F$ but varied a little with the operation conditions of the gun, where $W_F$ is the work function of the filament. The electron beam was decelerated to low energies just before it hit the sample. The elastically backscattered elec-

 ©2009 The American Physical Society

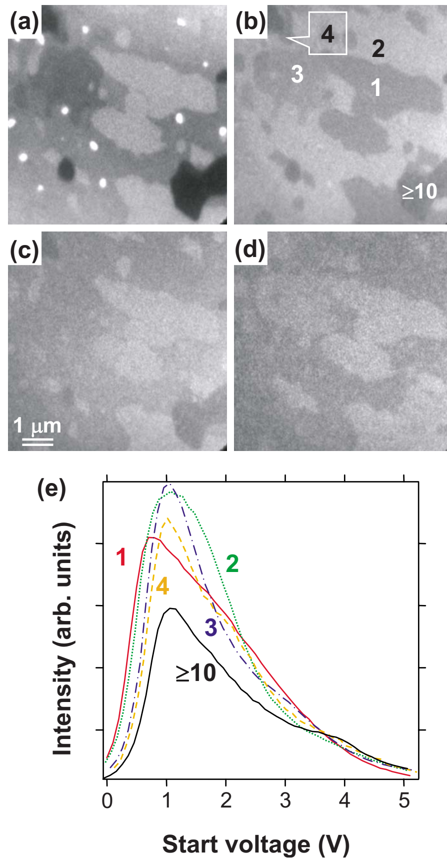


FIG. 1. (Color online) (a)–(d) SE PEEM images of epitaxial FLG grown on 6H-SiC(0001) taken at the start voltages $V_{ST}$ of 0.5, 1.5, 2.5, and 3.5 eV, respectively. (e) SE emission spectra obtained from the sequential SE PEEM images. Numbers in (b) and (e) indicate the number of graphene layers.

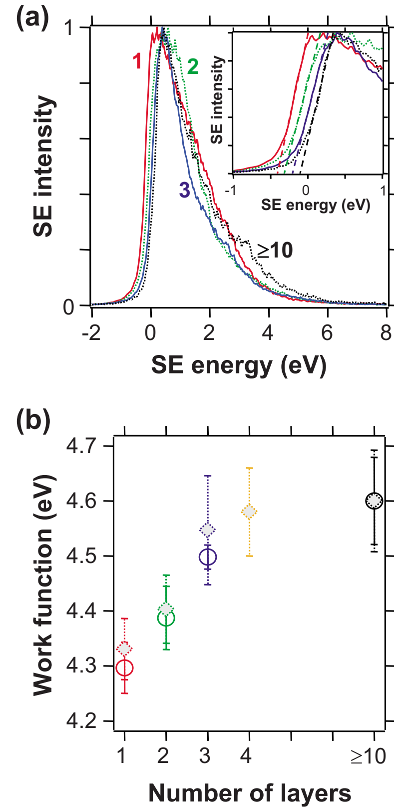


FIG. 2. (Color online) (a) SE emission spectra obtained in the dispersion mode. The selected-area aperture with the diameter of ~1 μm was located at areas with each number of graphene layers. Each spectrum is normalized by its maximum and minimum values (i.e., maximum to 1 and minimum to 0). The numbers correspond to the number of graphene layers. Inset shows the magnified spectra on which the tangential lines are overlaid as dashed lines. (b) Number-of-layers dependence of the work function. Circles and diamonds were obtained from the data in (a) and in Fig. 1(e). The error bars were obtained from the fitting errors of the tangential lines. We assumed that the work function of the thick graphene layers is equal to the reported value for bulk graphite, 4.6 eV.

trons from the sample were used to form LEEM images. Under the photon irradiation, photoelectrons emitted normal to the sample were accelerated to the energy $E^{PE}=e(V-V_{ST})+W_S+E_{KE}$, where $W_S$ is the work function of the sample and $E_{KE}$ is the "kinetic energy." We positioned an energy filter so as to let the elastically scattered electrons of $E^{beam}$ pass through it. The photoelectrons with the energy of $E^{PE}=E^{beam}$ formed PEEM images. The PEEM images at different kinetic energies were obtained by changing $V_{ST}$. The energy difference in each set of PES spectra was therefore precise, but there appeared practically uncontrollable shifts between energy axes of different sets of PES spectra such as those in Figs. 1(e) and 2(a) due to experimental details. However, this shift is of minor importance in this work because the absolute energy values are disregarded and only energy differences are discussed.

The epitaxial FLG was grown on 6H-SiC(0001) by annealing the samples at 1300–1500 °C in the commercial LEEM instrument (Elmitec LEEM III) at NTT. The number of graphene layers was microscopically determined using the quantized oscillation in the electron reflectivity.[4–6] The samples were taken out of vacuum and were transferred to the SPELEEM chamber in air. After introducing the samples into UHV, we annealed them at about 500 °C to remove adsorbates. The typical pressure during PEEM measurements was $1-3\times10^{-9}$ Torr. During the SPELEEM observations, the sample studied in this paper was kept above 150 °C because the samples became contaminated during PEEM observations at room temperature. This contamination could not be removed by annealing at 1200 °C, which suggests that it consisted of carbonaceous materials. All the PEEM images in this paper were obtained under irradiation by monochromatized synchrotron radiation at the energy of 400 eV.

## III. RESULTS AND DISCUSSION

Figures 1(a)–1(d) show SE PEEM images of epitaxial FLG grown on 6H-SiC(0001) taken at various start voltages $V_{ST}$. Numbers in Fig. 1(b) correspond to the number of graphene layers determined by LEEM. The graphene growth at higher temperatures caused larger pits at higher densities.[16] LEEM and cross-sectional transmission electron microscopy images indicated that thick graphene layers are

formed in the pits. LEEM can count the number of graphene layers up to about 10. Therefore, the graphene layers in the pit are numbered as $\geq 10$ in Fig. 1(b). Areas with different numbers of graphene layers can be discriminated in the SE PEEM images, but their relative intensities depend on the SE energy.

To understand the energy dependence of the SE PEEM images, the SE emission spectra were obtained from the sequential SE PEEM images as shown in Fig. 1(e). The SE emission spectra depend on the number of graphene layers in two aspects: the threshold start voltage of the SE emission and the spectrum shape. The threshold voltage corresponds to the vacuum level. Therefore, in Fig. 1(e), the work function increases with the number of graphene layers. The white dots in Fig. 1(a) correspond to the C-rich $6\sqrt{3}\times 6\sqrt{3}$ phase referred as the "0th" graphene layer.[11,13] The work function of the $6\sqrt{3}\times 6\sqrt{3}$ phase seems as small as or even smaller than that of the monolayer graphene. The work-function difference can also be estimated from the threshold energy of the total reflection of the electron beam and this type of measurement indicated that the difference seems to be at most 0.2 eV.

To investigate the number-of-layers dependence of the work function, we also measured SE emission spectra for monolayer, bilayer, trilayer, and thick layers in the dispersion mode. Figure 2(a) shows the measured SE emission spectra. In the dispersion mode, we observed the elastically scattered electrons with the energy of $E^{\mathrm{beam}}$ on the screen. The photoelectrons with the energy of $E^{\mathrm{PE}}$ were incident at different position on the screen. We determined $E^{\mathrm{PE}}$-$E^{\mathrm{beam}}$ from the distance between the elastically scattered electrons and photoelectrons. The horizontal axis in Fig. 2(a) is $E^{\mathrm{PE}}$-$E^{\mathrm{beam}}$ at $V_{\mathrm{ST}}=0$.

The work function was estimated from the intersections of tangential lines drawn on the low-energy cutoff of the SE emission spectrum with the zero intensity line. Such tangential lines are indicated by dashed lines in the inset of Fig. 2(a). The intersections should change with the number of graphene layers in the same way as the vacuum level. It has been reported that the work function of bulk graphite is 4.6 eV.[17] By assuming that the work function of the thick graphene layers is equal to this value, we obtained the number-of-layers dependence of the work function as shown in Fig. 2(b). From monolayer graphene to graphite, the vacuum level gradually increases by about 0.3 eV. Recently, Filleter *et al.*[18] determined the work-function difference between monolayer and bilayer graphenes grown on SiC using Kelvin probe force microscopy. They found that bilayer graphene increases the work function by 135 meV as compared to monolayer graphene This value is comparable to our result of about 0.1 eV.

Next, we investigate the number-of-layers dependence of the spectrum shape. Before doing so, however, we mention a difference between our SE emission spectra for epitaxial FLG and reported spectra for bulk graphite. It is well known that bulk graphite produces intense SE emission at around 3 eV above the vacuum level ($\sim$7.5 eV above the Fermi level).[19–24] In Figs. 1(e) and 2(a), however, there is no such intense emission line at this energy. The SE intensity map reconstructed from the two-dimensional SE emission patterns of epitaxial FLG did not exhibit such intense emission either.[15] We also measured energy spectra of SEs emitted by a 20 keV electron beam from graphene layers grown on SiC and highly oriented pyrolytic graphite (HOPG) using a scanning Auger microscopy instrument (Physical Electronics SAM670). We confirmed that, while HOPG produced a quite intense emission peak at around 3 eV above the vacuum level, no peak and a much weaker peak appeared at the same energy in the spectra from thin epitaxial FLG on the flat areas and from thick graphene layers in the pits, respectively. In fact, Figs. 1(e) and 2(a) certainly indicate that the thick graphene layers in the pit produce a weak peak on the high energy tail of the SE emission spectra, at about 2.8 eV higher than the main peak. We think that this weak peak has the same origin as the intense SE emission from bulk graphite, which would indicate that the results obtained by photon and electron irradiations are consistent.

It seems true that the intense SE emission line typical for bulk graphite is absent in the SE emission spectra from thin epitaxial FLG. However, we still do not completely understand the reason. The electron reflectivity from epitaxial FLG is generally low at 0–6 eV above the vacuum level,[4–6] which corresponds to high electron transmission through FLG. In addition, the escape depth of such low-energy electrons could be quite long.[25] Therefore, SEs emitted directly from thin epitaxial FLG would make a limited contribution to the measured spectra. The weakness of the SE peak from the thick graphene layers in the pits could also be due to their lower crystal quality, which would be supported by our atomic force microscopy result showing that the graphene layers in the pits undulate.

We have already shown that the electron reflectivity oscillates as functions of the electron energy and number of graphene layers.[4,5] In their pioneering work, Strocov and co-workers[26,27] clearly showed, using very-low-energy electron diffraction and density-functional-theory calculation, that the electron transmission (reflectivity) of graphite is strongly correlated with the band structure. The electron reflectivity from bulk graphite in the surface-normal direction is low up to about 6 eV above the vacuum level because bulk graphite has an unoccupied electronic band along the $\Gamma$-$A$ direction in this energy window,[4,26–28] where the reflectivity of epitaxial FLG oscillates. Bulk graphite has continuous electronic bands normal to the graphite sheet, but these bands split into discrete energy levels in FLG due to their finite thickness. When the energy of incident electrons coincides with one of the discrete energy levels, the electrons resonantly transmit through the layers, resulting in dips in the reflectivity.

Strocov *et al.*[26] showed that the electron transmission (reflectivity) data can be used to obtain the surface-projected dispersion map of the graphite band structure. Under the photon irradiation, some of the excited electrons are relaxed to the unoccupied states and are emitted into vacuum as secondary electrons. The SE emission should provide information about the unoccupied electronic structures. Actually, the calculated and measured dispersion maps[26] for graphite are quite similar to the SE intensity map for FLG.[15] This means that the reflectivity and SE emission are closely related via unoccupied electronic states. As for epitaxial FLG grown on

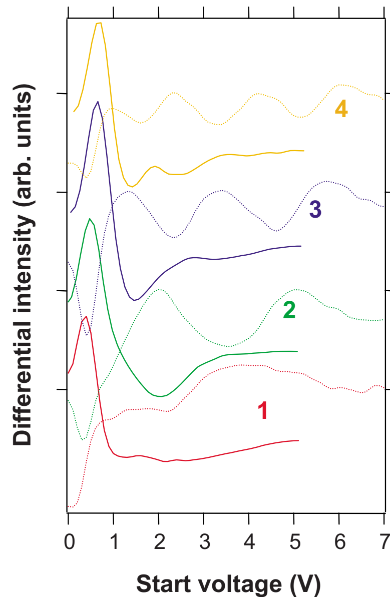


FIG. 3. (Color online) Number-of-layers dependence of the differential reflectivity spectra (dotted lines) and differential SE emission spectra (solid lines). The SE emission spectra in Fig. 1(e) were differentiated and smoothed. Each curve is shifted vertically for clarity.

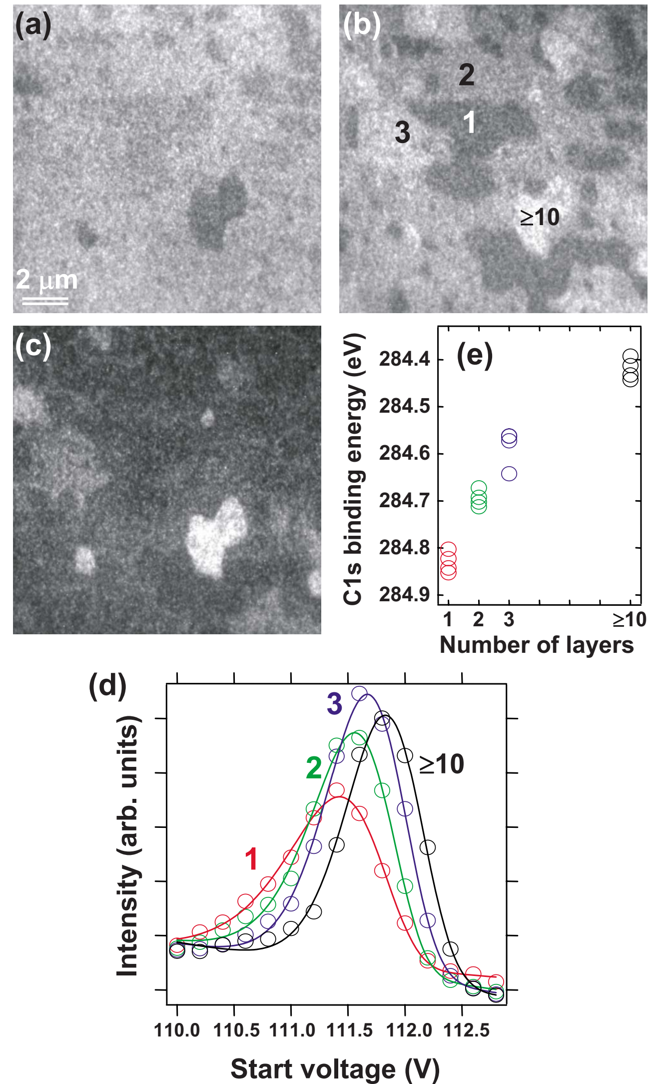


FIG. 4. (Color online) (a)–(c) C 1*s* PEEM images at the start voltage $V_{ST}$ of 111.4, 111.8, and 112.2 eV, respectively. The exposure time was 600 s for each image. The areas whose numbers of graphene layers are indicated are the same as in Fig. 1(b). (d) C 1*s* core-level spectra obtained from the sequential C 1*s* PEEM images. Open circles denote the experimental data and solid lines are the results of fitting the data to an asymmetric Gaussian function with a linear background. (e) Number-of-layers dependence of the C 1*s* binding energy. The peak start voltage was converted to the binding energy by assuming that the binding energy of the thick graphene layers is the same as that of bulk graphite, 284.42 eV.

SiC, the discrete energy levels in FLG could serve as the final states from which SEs are directly emitted and as the resonant states that facilitate the SE emission from the SiC substrate. The SE emission spectra in Figs. 1 and 2 should include structures related to these energy levels.

To confirm this, we compare the SE emission spectra to the reflectivity spectra. The reflectivity spectra exhibit clear oscillations at the start voltage between 0 and 7 V.[4–6] However, it is not easy to identify the oscillation in the SE emission spectra due to the high backgrounds. Therefore, we differentiated the reflectivity and SE emission spectra as shown in Fig. 3. The peak (dip) positions in the differential reflectivity spectra for bilayer to quadlayer reasonably match with the dip (peak) positions in the differential SE emission spectra. This indicates that the SE emission is high at the energy where the reflectivity is low. The monolayer graphene does not have clear structures in the differential spectra because the original spectra exhibit broad intensity changes. However, the SE emission spectra for monolayer graphene in Figs. 1(e) and 2(a) indicate that the SE intensities are considerably larger than those expected from the exponential decay at $V_{ST}=2-3$ eV, where a dip appears in the reflectivity spectra.[4–6] This high-and-low matching between the reflectivity and SE emission spectra reasonably suggests the SE emission from and/or through the discrete energy levels in FLG.

We further investigate C 1*s* PEEM images. The C 1*s* PEEM images in Fig. 4 indicate that regions with different numbers of layers are seen at different intensity levels. Figure 4(d) shows the C 1*s* PES spectra obtained from the sequential PEEM images. The PES spectra indicate that the start voltage (kinetic energy as well) of the maximum C 1*s* photoelectron intensity increases as the number of layers increases. This is consistent with the recent PES result on the evolution of the C 1*s* core-level spectrum upon graphene growth of up to 3.4 layers [Fig. 3(c) in Ref. 13]. This evolution also indicates that in the spectra for 0.9 and 1.2 monolayers of graphene, the signals due to the $6\sqrt{3}\times 6\sqrt{3}$ structure and SiC substrate are seen as shoulders and small peaks at the binding energy of about 1 eV lower and higher than the C 1*s* peak position of the 3.4-layer graphene, respectively.[13] Figure 4(d) indicates that the C 1*s* photoelectron intensity from monolayer graphene is higher than those from thicker

graphene at the start voltages of around 110.7 and 112.7 V, which clarifies that the PES spectrum for monolayer graphene includes photoelectrons from the $6\sqrt{3}\times 6\sqrt{3}$ structure and SiC substrate. However, their spectrum features are less prominent than those in the reported spectra for 0.9 and 1.2 monolayers of graphene.[13] To obtain the sequential PEEM images in Fig. 4, we used an energy filter with the width of 0.6 eV. Therefore, the spectra reconstructed from the images were worse in energy resolution than the reported ones, resulting in blurred spectrum features in Fig. 4(d). Additionally, the lower photon energy we used could lead to a higher surface sensitivity, which would reduce signals from the subsurface and substrate.

Here, we also have to mention recent PEEM results by Virojanadara *et al.*[29] They measured PEEM images of epitaxial FLG grown on SiC using Si $2p$ photoelectrons and showed that epitaxial FLG 1–4 layers thick can be discriminated in the images. In addition, they measured C $1s$ PES spectra for 1-$\mu$m$^2$-wide selected homogeneous areas with the thicknesses of 0.5, 1, and 3 layers. The spectra obtained using the photon energy of 450 eV were decomposed into three components corresponding to bulk SiC, graphene, and the $6\sqrt{3}\times 6\sqrt{3}$ structure. The intensity ratios of the components from graphene and the $6\sqrt{3}\times 6\sqrt{3}$ structure provide a good estimate of the number of graphene layers. Virojanadara *et al.*[29] also showed using conventional PES that the components from bulk SiC and the $6\sqrt{3}\times 6\sqrt{3}$ structure drastically decreased with the decrease in photon energy from 600 to 330 eV, which is consistent with the observed weak spectrum features from bulk SiC and the $6\sqrt{3}\times 6\sqrt{3}$ structure in Fig. 4.

To obtain the number-of-layers dependence of the C $1s$ core-level position, we determined the peak start voltages by fitting the spectra to an asymmetric Gaussian function with a linear background.[30] Solid lines in Fig. 4(d) are the fitting results. The peak start voltages were obtained for four different areas for each number of layers and were converted to the binding energies by assuming that the thick graphene layers have the same C $1s$ binding energy as bulk graphite, 284.42 eV.[13] Figure 4(e) shows the number-of-layers dependence of the C $1s$ binding energy. The C $1s$ binding energy of the monolayer graphene is about 0.4 eV lower than that of the thick graphene layers and it increases almost linearly except a slight concave behavior from monolayer to trilayer. Peak energies of core-level photoelectrons can shift for several reasons and a surface core-level shift and charge transfer from the substrate could be the reasons in this system. However, the reported C $1s$ spectra of natural graphite crystals and graphite films grown on SiC(0001) have only one component, which means that there is no surface core-level shift in the graphite surface.[31] The second component observed in highly oriented pyrolytic graphite, which was previously ascribed to the atoms in the surface layer,[32] is now believed to be associated with the lattice imperfections, most probably the microcrystal boundaries.[31] In any case, the second component appears at a lower binding energy than the main peak, which is not consistent with our result that FLG has higher binding energies than the thick graphene. Therefore, the charge transfer from the SiC substrate should explain the shift in the binding energy.[13] In fact, using ARPES, Ohta *et al.*[9] and Zhou *et al.*[10] reported that, for monolayer to bilayer to trilayer graphene, the Dirac point falls below the Fermi level by 0.44/0.40, 0.30/0.29, and 0.21/0.20 eV, respectively. These values are quite close to the shift in the C $1s$ binding energy between FLG and graphite, which completely fits the interpretation that the C $1s$ core levels in FLG are shifted due to charge transfer.

The C $1s$ core level and Dirac point move by almost the same values with the number of graphene layers. This means that the electronic band structures of FLG are rigid even under different levels of electron doping.[13] ARPES results of Ohta *et al.*[9] showed that the total number of electrons transferred to FLG is almost independent of the number of layers, which is consistent with the fact that the C-rich $6\sqrt{3}\times 6\sqrt{3}$ phase always exists at the graphene/SiC interface. The number of doped electrons in monolayer graphene is proportional to $(\Delta E)^2$, where $\Delta E$ is the shift of the Dirac point from the Fermi level. In $N$-layer graphene, the number roughly increases by factor $N$. Therefore, the constant number of doped electrons in FLG means that the shift of the Dirac point energy decreases with $\propto 1/\sqrt{N}$, which could explain the concave dependence seen in Fig. 4(e). More precise arguments require the calculation of the density of sates from the band structure. Ohta *et al.*[9] simulated the measured band structures near the $K$ point using the tight-binding calculation and showed that the constant number of doped electrons is consistent with the measured Dirac point shift.

We also found that the thinner graphene has lower work functions. Below, we will explain our attempt to understand this dependence, but complete understanding clearly requires further investigation. First, we note that the work function and C $1s$ binding energy change with the number of graphene layers rather similarly. Therefore, we assume that the vacuum level as well as the C $1s$ core level shift rigidly with the Dirac point. More strictly, however, the shift in the work function seems smaller than that in the C $1s$ binding energy. While the C $1s$ PES technique senses the graphene layers within the inelastic mean-free path, only the topmost graphene layer would be relevant to the vacuum level. Therefore, the vacuum level does not always shift by the same value with the C $1s$ core level. Simulations of the ARPES and scanning tunneling spectroscopy spectra using the tight-binding calculation showed that the on-site Coulomb energy is lower for deeper layers, which means that fewer electrons are doped in the topmost layer than in the deeper layers.[9,33] The on-site Coulomb energy at the topmost layer would determine the work function. As for the shift from the graphite value, the on-site Coulomb energy seems closer to the work function than the Dirac point energy, which may be evidence for the screening of the carrier in FLG. However, there still remains the difference between the on-site Coulomb energy and work function, especially for monolayer graphene, which suggests that other effects such as work function changes due to the surface/interface dipoles contribute to the number-of-layers dependence of the work function.

So far, we assumed that all the electronic structures of FLG are shifted rigidly by the charge transfer, which well explains the number-of-layers dependence of the C $1s$ core level and roughly explains that of the vacuum level. However, we found that this assumption contradicts with reported first-principles calculation results.[34] The calculation showed

that the work functions of SiC(0001)-graphene, SiC(0001)-2 graphene, and isolated graphene are 3.75, 4.33, and 5.11 eV, respectively.[34] From the viewpoint of the band structure, SiC(0001)-graphene and SiC(0001)-2 graphene correspond to the 0th graphene layer and monolayer graphene, respectively. The calculation reproduces the tendency for the thicker graphene to have larger work functions. However, while this calculation well reproduces the measured Dirac point shift of monolayer graphene, the calculated work-function difference between the monolayer graphene and isolated graphene is much larger than the experimental value between the monolayer and thick graphene. This calculation result suggests that the work function does not move in the same way as the Dirac point, which would mean that the charge distribution (dipole moments) at the surface/interface greatly influences the work function of FLG. Therefore, a precise interface structure is essential for calculating the work functions, but the calculation used a very simple model in which the $2\times2$ unit of graphene matches the $\sqrt{3}\times\sqrt{3}$ unit of SiC.[34] The complicated $6\sqrt{3}\times6\sqrt{3}$ structure is actually formed at the interface and could be largely different from the model used in the calculation.[13,35] The reported calculation also seems to overestimate the work-function difference between the 0th graphene layer and monolayer graphene,[34] which would also be due to this simple model structure. Calculations properly including the $6\sqrt{3}\times6\sqrt{3}$ structure are essential for understanding the number-of-layers dependence of the work function, which will clarify the applicability of the rigid-band model to FLG.

## IV. SUMMARY

In this paper, we investigated the number-of-layers dependence of electronic properties of epitaxial FLG using SPELEEM. Because the number of graphene layers can be determined digitally from the electron reflectivity measurements using LEEM, we can evaluate the electronic properties for each number of graphene layers. The SE PEEM images and SE emission spectra indicate that the work function increases with the number of graphene layers. The SE PEEM images are useful for determining the spatial distribution of the work function. The SE emission spectra also exhibit structures originating from the unoccupied states in FLG. Furthermore, we showed using the C 1*s* PEEM images that the C 1*s* core level shifts to lower binding energies as the number of graphene layers increases. The magnitudes of the shifts are very close between the C 1*s* core level and Dirac point, which supports the rigid-band model.

## ACKNOWLEDGMENTS

The authors thank M. Oura and T. Takeuchi for their help throughout the experiments. The synchrotron-radiation experiments were performed at SPring-8 with the approval of JASRI as part of the Senryaku Katuyou Program (Contract No. 2006B0180) and Juten Sangyo Riyo Program (Contract No. 2007A1919) of the Ministry of Education, Culture, Sports, Science and Technology. This work was partly supported by KAKENHI (Contract No. 19310085) from the Ministry of Education, Culture, Sports, Science and Technology of Japan.

[1] A. K. Geim and K. S. Novoselov, Nature Mater. **6**, 183 (2007).
[2] I. Forbeaux, J.-M. Themlin, and J.-M. Debever, Phys. Rev. B **58**, 16396 (1998).
[3] C. Berger, Z. Song, X. Li, X. Wu, N. Brown, C. Naud, D. Mayou, T. Li, J. Hass, A. N. Marchenkov, E. H. Conrad, P. N. First, and W. A. de Heer, Science **312**, 1191 (2006).
[4] H. Hibino, H. Kageshima, F. Maeda, M. Nagase, Y. Kobayashi, and H. Yamaguchi, Phys. Rev. B **77**, 075413 (2008).
[5] H. Hibino, H. Kageshima, F. Maeda, M. Nagase, Y. Kobayashi, Y. Kobayashi, and H. Yamaguchi, e-J. Surf. Sci. Nanotechnol. **6**, 107 (2008).
[6] T. Ohta, F. El Gabaly, A. Bostwick, J. L. McChesney, K. V. Emtsev, A. K. Schmid, T. Seyller, K. Horn, and E. Rotenberg, New J. Phys. **10**, 023034 (2008).
[7] T. Ohta, A. Bostwick, T. Seyller, K. Horn, and E. Rotenberg, Science **313**, 951 (2006).
[8] J. Algdal, T. Balasubramanian, M. Breitholtz, T. Kihlgren. and L. Walldén, Surf. Sci. **601**, 1167 (2007).
[9] T. Ohta, A. Bostwick, J. L. McChesney, T. Seyller, K. Horn, and E. Rotenberg, Phys. Rev. Lett. **98**, 206802 (2007).
[10] S. Y. Zhou, G.-H. Gweon, A. V. Fedorov, P. N. First, W. A. de Heer, D.-H. Lee, F. Guinea, A. H. C. Neto, and A. Lanzara, Nature Mater. **6**, 770 (2007).
[11] A. Bostwick, T. Ohta, J. L. McChesney, K. V. Emtsev, T. Seyller, K. Horn, and E. Rotenberg, New J. Phys. **9**, 385 (2007).
[12] A. Bostwick, T. Ohta, T. Seyller, K. Horn, and E. Rotenberg, Nature Phys. **3**, 36 (2007); E. Rotenberg, A. Bostwick, T. Ohta, J. L. McChesney, T. Seyller, and K. Horn, Nature Mater. **7**, 258 (2008); S. Y. Zhou, D. A. Siegel, A. V. Fedorov, F. El Gabaly, A. K. Schmid, A. H. C. Neto, D.-H. Lee, and A. Lanzara, Nature Mater. **7**, 259 (2008).
[13] K. V. Emtsev, F. Speck, Th. Seyller, L. Ley, and J. D. Riley, Phys. Rev. B **77**, 155303 (2008).
[14] F. Z. Guo, T. Muro, T. Matsushita, T. Wakita, H. Ohashi, Y. Senba, T. Kinoshita, K. Kobayashi, Y. Saitoh, T. Koshikawa, T. Yasue, M. Oura, T. Takeuchi, and S. Shin, Rev. Sci. Instrum. **78**, 066107 (2007).
[15] H. Hibino, H. Kageshima, F.-Z. Guo, F. Maeda, M. Kotsugi, and Y. Watanabe, Appl. Surf. Sci. **254**, 7596 (2008).
[16] V. Derycke, R. Martel, M. Radosvljevic, F. M. Ross, and Ph. Avouris, Nano Lett. **2**, 1043 (2002).
[17] T. Takahashi, H. Tokailin, and T. Sagawa, Phys. Rev. B **32**, 8317 (1985).
[18] T. Filleter, K. V. Emstev, Th. Seyller, and R. Bennewitz, Appl. Phys. Lett. **93**, 133117 (2008).
[19] R. F. Willis, B. Feuerbacher, and B. Fitton, Phys. Rev. B **4**, 2441 (1971).
[20] D. Marchand, C. Frétigny, M. Laguës, F. Batallan, Ch. Simon, I. Rosenman, and R. Pinchaux, Phys. Rev. B **30**, 4788 (1984).
[21] A. R. Law, M. T. Johnson, and H. P. Hughes, Phys. Rev. B **34**,

4289 (1986).
[22] L. S. Caputi, G. Chiarello, E. Colavita, A. Santaniello, and L. Papagno, Surf. Sci. **152–153**, 278 (1985).
[23] F. Maeda, T. Takahashi, H. Ohsawa, S. Suzuki, and H. Suematsu, Phys. Rev. B **37**, 4482 (1988).
[24] M. Breitholtz, J. Algdal, T. Kihlgren, S.-Å. Lindgren, and L. Walldén, Phys. Rev. B **70**, 125108 (2004).
[25] C. R. Brundle, J. Vac. Sci. Technol. **11**, 212 (1974).
[26] V. N. Strocov, P. Blaha, H. I. Starnberg, M. Rohlfing, R. Claessen, J.-M. Debever, and J.-M. Themlin, Phys. Rev. B **61**, 4994 (2000).
[27] N. Barrett, E. E. Krasovskii, J.-M. Themlin, and V. N. Strocov, Phys. Rev. B **71**, 035427 (2005).
[28] J.-C. Charlier, X. Gonze, and J.-P. Michenaud, Phys. Rev. B **43**, 4579 (1991).
[29] C. Virojanadara, M. Syväjarvi, R. Yakimova, L. I. Johansson, A. A. Zakharov, and T. Balasubramanian, Phys. Rev. B **78**, 245403 (2008).
[30] I. Kojima and M. Kurahashi, J. Electron Spectrosc. Relat. Phenom. **42**, 177 (1987).
[31] S. Lizzit, L. Petaccia, A. Goldoni, R. Larciprete, P. Hofmann, and G. Zampieri, Phys. Rev. B **76**, 153408 (2007).
[32] T. Balasubramanian, J. N. Andersen, and L. Walldén, Phys. Rev. B **64**, 205420 (2001).
[33] P. Lauffer, K. V. Emtsev, R. Graupner, Th. Seyller, L. Ley, S. A. Reshanov, and H. B. Weber, Phys. Rev. B **77**, 155426 (2008).
[34] A. Mattausch and O. Pankratov, Phys. Rev. Lett. **99**, 076802 (2007).
[35] C. Riedl, U. Starke, J. Bernhardt, M. Franke, and K. Heinz, Phys. Rev. B **76**, 245406 (2007).